Nicotinic pharmacophore: The pyridine N of nicotine and carbonyl of acetylcholine hydrogen bond across a subunit interface to a backbone NH

Angela P. Blum[a], Henry A. Lester[b], and Dennis A. Dougherty[a,1]

[a]Division of Chemistry and Chemical Engineering; and [b]Division of Biology, California Institute of Technology, Pasadena, CA 91125

This contribution is part of the special series of Inaugural Articles by members of the National Academy of Sciences elected in 2009.

Contributed by Dennis A. Dougherty, June 2, 2010 (sent for review April 1, 2010)

Pharmacophore models for nicotinic agonists have been proposed for four decades. Central to these models is the presence of a cationic nitrogen and a hydrogen bond acceptor. It is now well-established that the cationic center makes an important cation-π interaction to a conserved tryptophan, but the donor to the proposed hydrogen bond acceptor has been more challenging to identify. A structure of nicotine bound to the acetylcholine binding protein predicted that the binding partner of the pharmacophore's second component was a water molecule, which also hydrogen bonds to the backbone of the complementary subunit of the receptors. Here we use unnatural amino acid mutagenesis coupled with agonist analogs to examine whether such a hydrogen bond is functionally significant in the α4β2 neuronal nAChR, the receptor most associated with nicotine addiction. We find evidence for the hydrogen bond with the agonists nicotine, acetylcholine, carbamylcholine, and epibatidine. These data represent a completed nicotinic pharmacophore and offer insight into the design of new therapeutic agents that selectively target these receptors.

The nicotinic acetylcholine receptor (nAChR) is a pentameric, ligand-gated ion channel activated by the neurotransmitter acetylcholine (ACh), and also by nicotine and structurally related agonists (1–3). Nicotinic receptors mediate fast synaptic transmission at the neuromuscular junction of the peripheral nervous system. In addition, a family of paralogous nAChRs termed the neuronal receptors function in the central nervous system and certain autonomic ganglia, and the addictive and cognitive properties of nicotine are associated with these neuronal receptors (4, 5). Neuronal receptors comprised of α4 and β2 subunits are most strongly associated with nicotine addiction (6–9). They are upregulated during chronic nicotine exposure and are implicated in various disorders, including Alzheimer's disease and schizophrenia, and in protection against Parkinson disease. Interest in the development of molecules that selectively target α4β2 receptors has been growing, highlighted by the development of the smoking cessation drug, varenicline (6).

Many have undertaken the task of dissecting nicotinic agonists into a core pharmacophore, since the first publication on the topic in 1970 (10). While the details are debated, two aspects are clear. Nicotinic agonists contain a cationic nitrogen and a hydrogen bond acceptor (Fig. 1*A*) (11, 12). In 1990, we proposed that binding of the cationic nitrogen of acetylcholine would be mediated through a cation-π interaction with an aromatic residue of the nAChRs (13). We subsequently validated this model with the identification of a cation-π interaction to a conserved tryptophan residue for both acetylcholine and nicotine (14, 15). In fact, the cation-π interaction has been shown to be a general contributor to agonist affinity across the entire family of Cys-loop (pentameric) neurotransmitter-gated ion channels (16).

In the nAChRs, ligand binding occurs at the interface between adjacent principal (α4 in α4β2) and complementary (β2) subunits. Three segments from the α4 subunit (historically referred to as the A, B, and C "loops") form the principal face of the ligand-binding domain, which contains the cation-π binding site, and three segments from the β2 subunit (D, E, and F) form the complementary face. A major advance in the study of nAChRs was the discovery of the water-soluble acetylcholine binding proteins (AChBP) (17–22). AChBP serves as a structural template for the extracellular, N-terminal, ligand-binding domain of the nAChRs, sharing 20–24% sequence identity with the ligand-binding domain of the much larger ion channel proteins. Several AChBP structures with ligands bound have been published, including structures of AChBP in complex with the ACh analog carbamylcholine (CCh) and with nicotine (18) and the nicotine analog epibatidine (21). Drugs that target the nAChR, such as nicotine and epibatidine, typically contain a protonatable amine rather than the quaternary ammonium seen in ACh. Along with the cation-π interaction, the crystallography indicated a hydrogen bond between the N^+H and the backbone carbonyl of the tryptophan that also forms the cation-π interaction, and functional studies on intact receptors confirmed the hydrogen bonding interaction (14, 23).

Concerning the second component of the pharmacophore, the hydrogen bond acceptor, the AChBP structure produced intriguing results. With nicotine bound, the pyridine nitrogen makes a hydrogen bond to a water molecule that is positioned by hydrogen bonds to the main chains of two residues, the CO of N107 and the NH of L119, both in the complementary subunit (α4β2

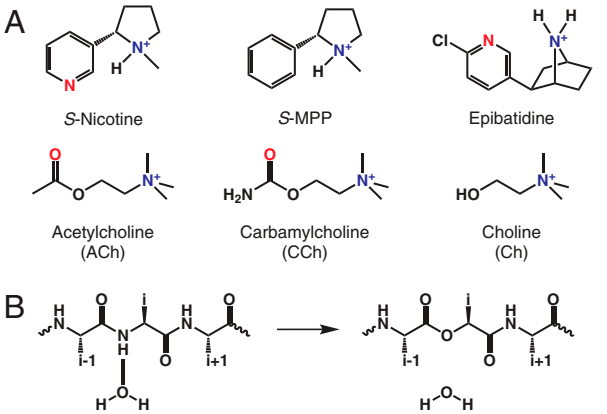

Fig. 1. Key structures considered in the present work. (*A*) Structures of agonists used. Hydrogen bond acceptor moieties are red and cationic nitrogens are blue. (*B*) Backbone amide to ester mutation strategy for perturbing a hydrogen bond.

Author contributions: A.P.B. and D.A.D. designed research; A.P.B. performed research; A.P.B., H.A.L., and D.A.D. analyzed data; and A.P.B., H.A.L., and D.A.D. wrote the paper.

The authors declare no conflict of interest.

See Commentary on page 13195.

[1]To whom correspondence should be addressed. E-mail: dadougherty@caltech.edu.

This article contains supporting information online at www.pnas.org/lookup/suppl/doi:10.1073/pnas.1007140107/-/DCSupplemental.

numbering; residues are in the β2 sequence FYSNAVVSYDGSIFWLPPA) (Fig. 2) (18). In other structures, including those with CCh or epibatidine bound, the overall binding site structure is preserved, although the key water molecule is not always evident, especially in lower-resolution structures.

A key question, then, is the extent to which predictions based on the AChBPs, which evolved to bind a target molecule, relate to the nAChRs, which evolved to undergo a global structural change (to gate) on binding ACh. Here we describe an approach to probe with high precision a specific structural interaction in a complex receptor protein. Using unnatural amino acid mutagenesis and agonist analogs, we find that nicotine, acetylcholine, epibatidine, and carbamylcholine make the same hydrogen bond involving the backbone NH of β2L119 of the α4β2 receptor, supporting a common pharmacophore for acetylcholine and nicotine.

Results

Strategy. A well-established strategy for probing potential backbone hydrogen bonds is to replace the residue that contributes the hydrogen bond donor with its α-hydroxy analog (Fig. 1*B*) (24–28). This mutation converts a backbone amide to a backbone ester, a subtle change that impacts backbone hydrogen bonding in two ways. The backbone NH that can donate a hydrogen bond is removed, and the carbonyl oxygen, by virtue of being part of an ester rather than an amide, is a weaker hydrogen bond acceptor.

In the present context, simply seeing a change in receptor function in response to appropriate backbone ester substitutions would not prove the presence of the proposed interaction. Backbone mutation is certainly subtle, but when installed in an important region of the receptor it could affect function in a number of ways. As such, we sought a way to provide a direct connection between any consequences of backbone mutation and the proposed hydrogen bond. To do this, we considered the molecule *S*-*N*-methyl-2-phenylpyrrolidine (*S*-MPP, Fig. 1*A*). In this structure a phenyl ring replaces the pyridyl group of nicotine, obliterating the possibility of forming the proposed hydrogen bond. This would allow a "double mutant cycle" analysis that links the backbone NH to the pyridine N. If the mutant cycle analysis shows that the effects of the two changes—the backbone mutation and the modification of the drug—are substantially nonadditive, this would provide compelling evidence for the proposed interaction.

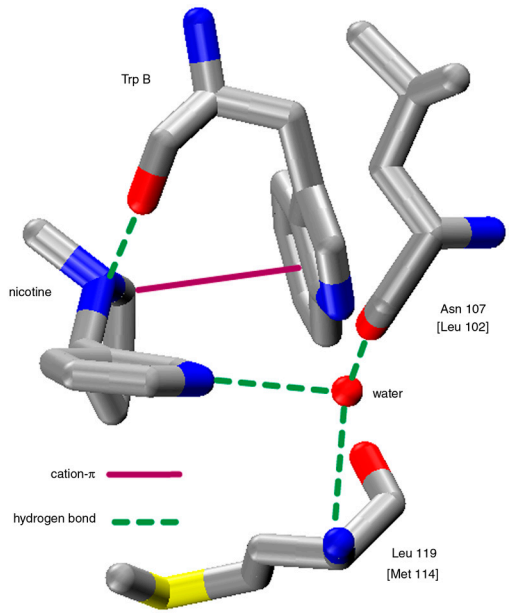

Fig. 2. Key interactions seen in the crystal structure of nicotine bound to AChBP (PDB ID code 1UW6). Residue numbering is for the α4β2 receptor, with AChBP homologs in brackets.

The metric used to evaluate receptors is EC_{50}, the effective concentration of agonist required to achieve half-maximal response. This is a functional measure that can be influenced by changes to drug binding and/or efficacy of activation of the receptor. Previously we have shown that subtle mutations to TrpB of the binding site primarily, if not exclusively, affect agonist binding (14), but we cannot assume the same for Leu119. Because the goal here is to map the pharmacophore for a collection of agonists, we are interested in factors that influence receptor activation. We consider EC_{50} to be an appropriately useful guide for understanding agonism and designing new agonists, but more detailed studies of the mutations considered here would be valuable.

Optimization of Nonsense Suppression Experiments. The α4β2 receptor is a pentamer with two possible stoichiometries, $(\alpha4)_2(\beta2)_3$ and $(\alpha4)_3(\beta2)_2$ termed A2B3 and A3B2, respectively. Our studies have focused on the A2B3 receptor, which shows the higher sensitivity to nicotine and is thought to be upregulated during chronic nicotine exposure. Subunit stoichiometry can be managed by controlling mRNA injection ratios. Exclusive expression of A2B3 can be verified by monitoring I-V relationships of agonist-induced currents, as described previously (14).

This study represents the first report of unnatural amino acid mutagenesis in the β2 subunit of α4β2. Since nonsense suppression often produces low protein yields of the subunit where the suppression occurs, it was critical to ensure that a receptor with excess β2 subunit, i.e., the A2B3 stoichiometry, was exclusively produced in nonsense suppression experiments. To that end, mRNA ratios substantially favoring the β2 subunit were explored. We found that an injected mRNA ratio of 1:20 of $\alpha4:\beta2$ (with β2 containing the nonsense suppression site) gave I-V relationships indicative of A2B3 (14), while still providing enough current to conduct meaningful dose-response experiments. The α4 subunit also contained a known mutation in the M2 transmembrane helix (L9'A), which improves receptor expression and lowers whole-cell EC_{50} values, but does not influence the binding trends of the receptor (29).

One challenge in incorporating a hydroxy acid at β2L119 was to limit the amount of current observed from oocytes injected with full length tRNA that was not synthetically appended to an amino or α-hydroxy acid. Such current would indicate that the suppressor tRNA was aminoacylated by an endogenous aminoacyl-tRNA synthetase and delivered a natural amino acid at the mutation site. We observed significant background currents attributable to such infidelity when using the suppressor tRNA THG73, which has been the workhorse of our unnatural amino acid mutagenesis experiments (30). Employing the recently developed opal suppressor tRNA TQOpS' (31, 32) significantly reduced this background current at β2L119. Aminoacylation from TQOpS' was assessed for each agonist by injection of unacylated TQOpS', and full dose-response relations were generated for agonists displaying >20 nA of current. Suppression experiments typically produced ≥1 μA of current and yielded Hill and EC_{50} values that were markedly different from unacylated TQOpS' control experiments, and so the small background currents are not expected to distort the reported EC_{50} values. With these conditions, characterization of mutant receptors was straightforward (Fig. 3).

Amide to Ester Backbone Mutation at β2L119 Impacts Receptor Function. To probe the hydrogen bond suggested by the AChBP structures, β2L119 was replaced with its α-hydroxy analog (leucine, α-hydroxy; Lah). Meaningful increases in EC_{50} for the backbone amide to ester mutation were seen for the conventional agonists nicotine, ACh, CCh, and epibatidine, suggesting a signif-

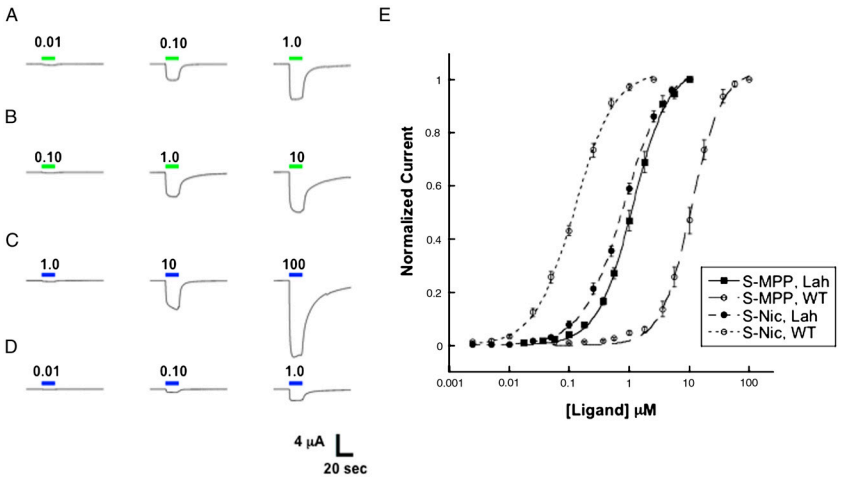

Fig. 3. Representative current waveforms and dose-response relations for *S*-nicotine and *S*-MPP. Agonist-induced current waveforms for (*A*) *S*-Nic on wild-type α4β2. (*B*) *S*-Nic on α4β2L119Lah. (*C*) *S*-MPP on wild-type α4β2. (*D*) *S*-MPP on α4β2L119Lah. Concentrations are in μM. (*E*) Dose-response relations for *S*-Nic and *S*-MPP on wild-type α4β2 or α4β2L119Lah.

icant functional role for the backbone NH (Table 1 and Fig. 3). In contrast, no shift was seen for the very weak agonist choline.

As noted above, we considered *S*-MPP as a potentially informative structure for probing the pyridine hydrogen bond. As such, we adapted existing synthetic protocols (33) to prepare *N*-methyl-2-phenylpyrroline (MPP). Recrystallization of the dibenzoyl tartrate salt (at the phenylpyrrolidine stage) gave the *S* enantiomer.

As expected, *S*-MPP is a much poorer agonist than nicotine, showing a ~120-fold higher EC_{50} with the wild-type receptor. For nicotine, the *S* enantiomer is the higher affinity enantiomer and the one traditionally used in studies of nicotinic receptors. We find that *S*-MPP has a twofold lower EC_{50} than racemic MPP, indicating that the higher affinity enantiomer is being used.

Incorporation of a backbone ester at β2L119 leads to a remarkable change in relative agonist potencies. Instead of the increase in EC_{50} seen with nicotine, *S*-MPP actually shows a *decrease* in EC_{50}; *S*-MPP is a more potent agonist when the backbone ester is present than when the natural backbone amide is present. In fact, when the backbone ester is present, nicotine and *S*-MPP display comparable potency.

Table 1. EC_{50} values, Hill coefficients, and relative efficacies*

Agonist	Mutation	EC_{50}, nM	n_H
S-Nic	WT	120 ± 5	1.3 ± 0.05
	Leu	120 ± 3	1.5 ± 0.05
	Lah	800 ± 30	1.3 ± 0.04
S-MPP	WT	11,000 ± 400	1.7 ± 0.08
	Leu	14,000 ± 900	1.5 ± 0.11
	Lah	1,100 ± 40	1.5 ± 0.05
ACh	WT	360 ± 20	1.3 ± 0.07
	Leu	440 ± 20	1.3 ± 0.08
	Lah	3,000 ± 100	1.2 ± 0.04
CCh	WT	7,200 ± 80	1.3 ± 0.02
	Leu	7,900 ± 200	1.2 ± 0.03
	Lah	29,000 ± 800	1.2 ± 0.04
Ch	WT	140,000 ± 4,000	1.6 ± 0.06
	Leu	140,000 ± 20,000	1.2 ± 0.09
	Lah	150,000 ± 5,000	1.4 ± 0.05
Epi	WT	0.79 ± 0.04	1.4 ± 0.07
	Leu	0.58 ± 0.05	1.5 ± 0.15
	Lah	2.9 ± 0.06	1.3 ± 0.03

*All studies showed current values at +70 mV, normalized to −110 mV, ≤0.08, confirming the A2B3 stoichiometry. Errors are standard error of the mean. Epi is epibatidine. Mutations identified as "Leu" represent recovery of the wild-type receptor by nonsense suppression.

The AChBP structure also predicts that a second residue in the complementary subunit positions the water molecule in proximity to the pyridine N of nicotine. The backbone carbonyl of β2N107 is expected to make a hydrogen bond to the water molecule in conjunction with the first hydrogen bond made by β2L119 (Fig. 2). As noted above, an established strategy for attenuating the hydrogen bonding ability of a backbone carbonyl is to mutate the $(i + 1)$ residue to its α-hydroxy acid (Fig. 1*B*). However, nonsense suppression experiments at the β2A108 site gave inconsistent results that suggested we could not reliably control the stoichiometry of the mutant receptor. As such, we have been unable to probe this interaction.

Mutant Cycle Analyses Indicate Strong Receptor-Agonist Interactions at β2L119. As noted above, a mutant cycle analysis (Fig. 4) is the standard way to determine whether pairs of mutations are independent or are coupled. EC_{50}-based mutant cycle analyses have been performed by our lab and others to investigate multiple interactions in Cys-loop receptors and related structures (28, 34–36). For several different agonist pairs, coupling coefficients (Ω) and coupling energies (ΔΔG) were calculated (Table 2).

Mutant cycle analysis for the *S*-nicotine/*S*-MPP pair and the β2L119/β2L119Lah pair predicts a substantial coupling energy of 2.6 kcal/mol. This is a relatively large energy for a putative hydrogen bond, and it provides strong evidence for a hydrogen bonding interaction between the pyridine N of nicotine and the backbone NH of β2L119.

We also considered double mutant cycle analyses for the agonists ACh and CCh using choline as the reference compound, as it lacks the key hydrogen bond acceptor. This is a much less subtle probe than the *S*-nicotine/*S*-MPP pair, but it still could produce relevant results. Indeed, we find that for both the ACh/Ch and CCh/Ch pairs, smaller, but still meaningful, coupling energies are seen (Table 2).

Discussion

The nicotinic receptor has produced one of the longest-known, best-studied pharmacophores. The original study of Beers and Reich (10) proposed that two points, a cationic nitrogen and a hydrogen bond acceptor, were required for successful interaction with biological receptors. Later discussion debated the optimal distance between the two points (deemed the internitrogen distance), and more recent models have alluded to pharmacophore binding partners within the biological receptors. Despite 40 years of interest in the nicotinic pharmacophore, the binding partners of the essential two point pharmacophore have only recently been identified. Pioneering mutagenesis and affinity labeling studies of

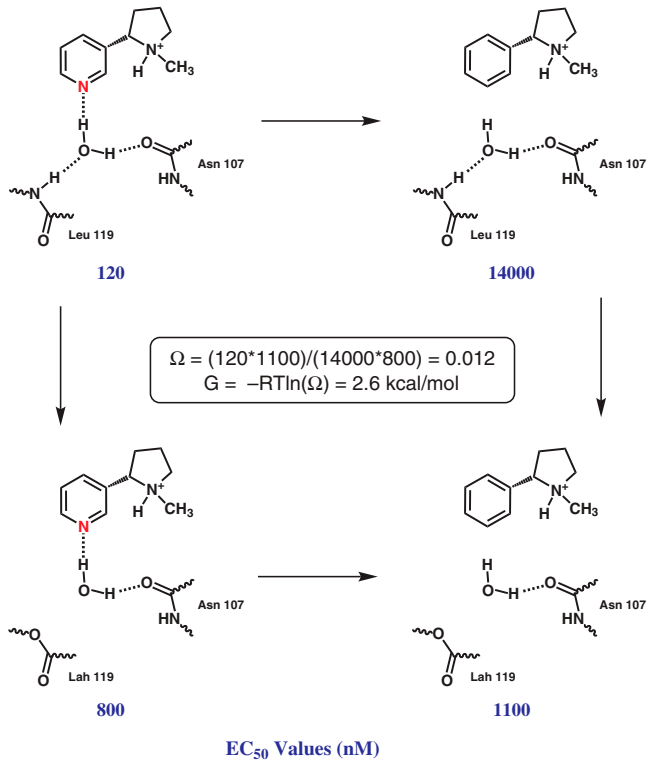

Fig. 4. Double mutant cycle analysis for *S*-Nic and *S*-MPP on wild-type α4β2 and α4β2L119Lah.

the receptor from *Torpedo* rays identified a number of aromatic amino acids near the binding site (1, 3). Early unnatural amino acid mutagenesis studies showed that one of these aromatics, now termed TrpB, makes a cation-π interaction with ACh in the muscle-type nAChR (15), and more recent studies established a comparable interaction to both ACh and nicotine in the α4β2 receptor (14).

The search for the presumed hydrogen bond donor to the acetyl group of ACh and the pyridine N of nicotine was much more challenging. A breakthrough came with the discovery of the AChBPs, and in 2004 a structure of nicotine bound to AChBP was reported (18). As shown in Fig. 2, that AChBP structure confirmed the cation-π interaction to TrpB. It also implicated a hydrogen bond between the pyrrolidine N^+H and the backbone carbonyl of TrpB, an interaction that was subsequently confirmed by unnatural amino acid mutagenesis (14, 23).

Importantly, the AChBP structure also suggested the binding partner for the second element of the pharmacophore. In AChBP, the pyridine N of nicotine makes a water-mediated hydrogen bond to a backbone NH and to a backbone carbonyl (Fig. 2). This elegant arrangement emphasizes the interfacial nature of the agonist binding site, as the pyridine N interacts with residues that are on the complementary subunit, while TrpB, which makes the cation-π interaction and the hydrogen bond to the pyrrolidine N^+H, lies in the principal subunit. The value of AChBP in guiding nAChR research is undeniably large, especially in the present context. It would have been very challenging to guess the hydrogen bond partner(s) to agonists such as ACh and nicotine before the structure of AChBP with nicotine bound. Nevertheless, AChBP is not a nAChR. AChBP evolved to bind ligands, not to gate an ion channel in response to ACh binding. As such, tests of predictions from AChBP structures in real receptors are always essential.

Table 2. Coupling parameters (Ω) and ΔΔG values for mutant cycle analyses

Agonist	Ω	ΔΔG, kcal mol^{-1}
S-Nic/*S*-MPP	0.012	2.6
ACh/Ch	0.16	1.1
CCh/Ch	0.29	0.73

Here we employ a unique strategy to test the water-mediated hydrogen bonding model of Fig. 2 in the neuronal, α4β2 nAChR. The α4β2 receptor shows high affinity for nicotine, and it is generally accepted to be the dominant receptor subtype that contributes to nicotine addiction. Our studies of α4β2 are made possible by recent advances (14) that allow us to express significant quantities of α4β2 in *Xenopus* oocytes, to control subunit stoichiometry, and to efficiently incorporate unnatural amino acids into the receptor. Recently, we have shown that the cation-π interaction and the hydrogen bond to TrpB are strong in the $(\alpha 4)_2(\beta 2)_3$ receptor (14).

To probe the second hydrogen bond suggested by AChBP, we mutated β2L119 to its α-hydroxy analog. This removes the critical NH, and, indeed, the agonists nicotine, ACh, CCh, and epibatidine, all show 5- to 7-fold increases in EC_{50} in response to the mutation. While consistent with the hydrogen bonding model, these observations certainly do not prove it. It could be that the backbone mutation is simply generically disruptive to receptor function.

To make an explicit connection between the pyridine N of nicotine and the backbone NH of β2L119, we combined backbone mutagenesis with a modification of the agonist, removing the pyridine N to create *S*-MPP. Of course, *S*-MPP would never be the target of a medicinal chemistry study; it can be anticipated to be a terrible drug at the nAChR. Here it is used as a chemical probe, to evaluate a key binding interaction of the potent drug nicotine.

Studies with *S*-MPP produced remarkable results. As expected, it is a very poor agonist at the wild-type receptor. However, completely opposite to what is seen with nicotine, ACh, CCh, or epibatidine, introduction of the backbone ester at β2L119 *lowers* EC_{50} for *S*-MPP. In fact, *S*-MPP and nicotine are comparably potent at the mutant receptor. Clearly the backbone mutation has had dramatically different effects on the two agonists. The effect can be quantified by a mutant cycle analysis, which reveals a coupling energy of 2.6 kcal/mol between the backbone mutation and the agonist "mutation." This is a quite substantial energy, especially when one considers that these chemical changes—both in the protein and in the ligand—are more structurally subtle than those typically employed in mutant cycle analysis studies using conventional mutagenesis.

The results with *S*-MPP provide strong support for the nicotine binding model based on the AChBP structure. As noted above, however, AChBP structures with CCh or epibatidine bound do not include the key water molecule, although other components of the hydrogen bonding network are comparably positioned. We find that ACh, CCh, and epibatidine all respond to the backbone ester mutation in a way that is comparable to that seen for nicotine. In addition, choline, a weak agonist that lacks the hydrogen bond acceptor of ACh and CCh, is not influenced by the backbone mutation. We thus conclude that all the drugs studied here make a hydrogen bonding interaction with the backbone NH of β2L119; the nicotinic pharmacophore has thus been completed by interactions with the complementary subunit. Note that these studies do not establish that the interaction between the hydrogen bond acceptor component of the agonists and the backbone NH of β2L119 is mediated by a water molecule; a direct interaction would be just as compatible with our data. At present, we feel the water-mediated interaction is the most reasonable interpretation, but further experiments to address this point would be valuable.

We have now used chemical-scale investigations of functional receptors to establish a three-point interaction between nicotine

and the α4β2 neuronal nAChR, the receptor most strongly associated with nicotine addiction. A cation-π interaction to TrpB has been established by progressive fluorination of the key tryptophan. Backbone mutagenesis has been used to establish two key hydrogen bonds: the pyrrolidine N^+H hydrogen bonds to the backbone carbonyl of TrpB and the pyridine N of nicotine hydrogen bonds to the backbone NH of β2L119. Studies of these two hydrogen bonds were inspired by the AChBP structures, emphasizing the substantial impact of AChBP on nAChR research.

At the same time, AChBP is not a neurotransmitter-gated ion channel; it evolved to serve a different function than a nAChR. As such, we should anticipate some differences between the two structures. Indeed, two features of the nicotine-AChBP structure have been shown to be not functionally significant in studies of nAChRs. The AChBP structure clearly shows a cation-π interaction between the CH_3 of nicotine and a tyrosine at the agonist binding site termed TyrC2 (Fig. S1) (18). This methyl group—which carries a charge comparable to a CH_3 attached to the N^+ of ACh—points directly at the center of the aromatic ring of TyrC2 and essentially makes van der Waals contact with the ring, unquestionably a cation-π interaction. However, we find no experimental support for this cation-π interaction in either the muscle-type or the α4β2 nAChR. In each system, inserting 4-CN-Phe at TyrC2 gives essentially wild-type receptor function (14, 15). A CN group is very strongly deactivating in a cation-π interaction, and so this result is in conflict with the AChBP structure. Note that in a different Cys-loop receptor, the residue at position C2 does make a functionally significant cation-π interaction to the natural agonist serotonin (37).

In addition, all AChBP structures—the nicotine, CCh, and epibatidine bound structures considered here as well as the "apo" structure—contain a strong hydrogen bond between the indole NH of TrpB and the backbone carbonyl of the residue that corresponds to β2L119 (Fig. S1). N • • • O distances range from 2.7 to 3.0 Å. However, earlier studies of the muscle-type receptor found no evidence for an important interaction of this kind. In particular, TrpB can be substituted by unnatural amino acids in which the indole ring is replaced by a naphthalene or an *N*-methylindole with very little impact on EC_{50} (15). All of these analogs lack the critical hydrogen bond-donating NH of the Trp indole ring.

In summary, we have used a combination of unnatural amino acid mutagenesis and chemical synthesis to provide strong evidence for a functionally important hydrogen bond between the pyridine N of nicotine and the backbone NH of β2L119 in the nicotine-sensitive α4β2 receptor. A similar interaction contributes to the binding of ACh, CCh, and epibatidine. We have now used unnatural amino acid mutagenesis to establish three strong contact points between this critical receptor and nicotine: the cation-π interaction to the side chain of TrpB, the hydrogen bond between the pyrrolidine N^+H and the backbone carbonyl of TrpB, and the hydrogen bond between the pyridine N and the backbone NH of β2L119. There is much interest in the pharmaceutical industry in developing subtype-selective agonists of neuronal nAChRs, and it seems likely that the complementary subunit will play the dominant role in discriminating among subtypes. As such, these studies of a key binding interaction involving the complementary binding site suggest a general strategy for developing insights that could lead to subtype-specific pharmaceuticals.

Materials and Methods

Molecular Biology Protocols. Rat α4 and β2 cDNA in the pAMV vector was linearized with the restriction enzyme Not 1. mRNA was prepared by in vitro transcription using the mMessage Machine T7 kit (Ambion). Unnatural mutations were introduced by the standard Stratagene QuickChange protocol, using a TGA mutation at the site of interest. The α4 subunit contained a known mutation in the M2 transmembrane helix (L9′A) that improves receptor expression and lowers whole-cell EC_{50} values, but does not influence the ligand-binding trends of the receptor (29). Stage V–VI *Xenopus laevis* oocytes were injected with mRNA in a 1:1 or 1:20 ratio of α4L9′A:β2 for wild-type experiments or suppression with α-hydroxy acids, respectively. Hydroxy or amino acids were appended to the dinucleotide dCA and enzymatically ligated to the truncated 74-nucleotide TQOpS′ tRNA as previously described (30). Each cell was injected with 75 nL of a 1:1 mixture of mRNA (20–25 ng of total mRNA): tRNA (20–30 ng), with oocytes injected with Leu ligated to TQOpS′ receiving an additional 75 nL after 24 h of incubation at 18 °C. Wild-type recovery experiments (injection of tRNA appended to the natural amino acid) were performed to evaluate the fidelity of the unnatural suppression experiments. Additional controls, mRNA only and 74-mer TQOpS′ ligated to dCA (TQOpS′-dCA), were also examined. While small currents (typically less than 200 nA) were seen for TQOpS′-dCA control experiments, EC_{50} and Hill values were substantially different from suppression values.

Electrophysiology Protocols. Electrophysiology experiments were performed 24–48 h after injection using the OpusXpress 6000A instrument (Axon Instruments) in two-electrode voltage clamp mode at a holding potential of −60 mV. The running buffer was Ca^{2+}-free ND96 solution (96 mM NaCl, 2 mM KCl, 1 mM $MgCl_2$, and 5 mM Hepes, pH 7.5). During typical recordings, agonists were applied for 15 s followed by a 116-s wash with the running buffer. For recordings with epibatidine, the first eight drug concentrations were applied for 90 s with a 116-s wash with running buffer, while the remaining concentrations were applied for 15 s with a 116-s wash. Dose-response data were obtained for ≥8 agonist concentrations on ≥6 cells. All EC_{50} and Hill coefficient values were obtained by fitting dose-response relations to the Hill equation and are reported as averages ± standard error of the fit. A detailed error analysis of nonsense suppression experiments reveals data are reproducible to ±50% in EC_{50} (38, 39). Voltage jump experiments were conducted to verify stoichiometry as described previously (14).

Double mutant cycle analyses were performed with EC_{50} values to calculate coupling coefficients (Ω) using the equation $\Omega = (EC_{50}^{\text{Leu,ligand}} \bullet EC_{50}^{\text{Lah,ligand analog}})/(EC_{50}^{\text{Leu,ligand analog}} \bullet EC_{50}^{\text{Lah,ligand}})$, where Leu, ligand and Leu, ligand analog represent the EC_{50} of the wild-type receptor with either ligand and Lah, ligand; and Lah, ligand analog represent the EC_{50} of the ester mutation with either ligand. Coupling energies $\Delta\Delta G_{int}$ were calculated from the equation $\Delta\Delta G_{int} = -RT\ln\Omega$.

Synthesis of *N*-Methyl-2-Phenylpyrrolidine Hydrochloride. Racemic 2-phenylpyrrolidine (5.0 g, 34 mmol), prepared according to a published protocol (33), was mixed with dibenzoyl-*L*-taratric acid (6.1 g, 17 mmol) in a 100-mL round-bottom flask equipped with a reflux condenser. To this was added 35% ethanol in ethylacetate (30 mL). The solution was heated to boiling for 10 min and then cooled to room temperature overnight. The white crystals were collected, rinsed with cold ethylacetate, and then submitted to five sequential recrystallizations. The yield was (10%, 2.2 g). Spectral data are ^{1}H NMR ($CDCl_3$, 300 MHz) δ 8.20 (4H, m), 7.61–7.32 (16H, m), 5.92 (2H, s), 5.03 (4H, b), 4.54 (2H, dd, J = 9.1, 6.7 Hz), 3.38 (4H, m), 2.27–2.00 (8H, m); ^{13}C NMR ($CDCl_3$, 75 MHz) δ 172.58, 166.45, 134.91, 132.73, 130.54, 129.70, 128.83, 128.76, 128.03, 127.37, 75.60, 62.74, 44.80, 30.42, 23.37. High resolution mass spectrometry (HRMS) (FAB+) m/z calculated for $C_{10}H_{14}N$ [M+]: 148.1126, found 148.1081. To obtain enantioenriched 2-phenylpyrrolidine, the product was vigorously stirred in a 1:1 mixture of 2 M NaOH: CH_2Cl_2. The organic layer was then extracted with additional CH_2Cl_2 (3×), washed with brine, dried over Na_2SO_4, and concentrated to yield enantioenriched 2-phenylpyrrolidine as a yellow oil (yield: 95%). NMR spectra are consistent with previously reported data. HRMS (FAB+) m/z calculated for $C_{10}H_{14}N$ [M + H]: 148.1126, found 148.1134. To establish enantiomeric excess, the product was converted to ethyl 2-phenylpyrrolidine-1-carboxylate via a previously described procedure (40), and this material was evaluated by analytical chiral HPLC analysis using a Chiralcel OD-H column (4.6 mm × 25 cm) from Daicel Chemical Industries, Ltd., with 2% isopropyl alcohol in hexanes, giving an enantiomeric excess of 96%. ^{1}H NMR of ethyl 2-phenylpyrrolidine-1-carboxylate gave (CH_3OD, 300 MHz) δ; 7.32–7.15 (5H, m), 4.92 (1H, m), 4.08 (IH, m), 3.92 (1H, m), 3.59 (2H, q, J = 7.7 Hz), 2.34 (1H, m), 1.95–1.86 (4H, m), 1.26 (1H, t, J = 7.0 Hz), 0.94 (1H, t, J = 7 Hz); ^{13}C NMR of ethyl 2-phenylpyrrolidine-1-carboxylate ($CDCl_3$, 75 MHz) δ 155.40, 144.32, 128.22, 126.59, 125.44, 60.85, 47.34, 47.03, 35.71, 23.58, 14.79. HRMS of ethyl 2-phenylpyrrolidine-1-carboxylate (FAB+) m/z calculated for $C_{13}H_{18}O_2N$ [M + H]: 220.1338, found 220.1336.

Enantioenriched 2-phenylpyrrolidine from above, (0.13 g, 0.86 mmol) was added to a two-neck, 25-mL round-bottom flask equipped with a reflux condenser. To this was added 4 mL of formic acid and 2 mL of 37 wt% formaldehyde (in H_2O). The mixture was stirred and heated to reflux at

80 °C for 3 h. The solution was cooled to room temperature and made basic (pH 12) by the addition of 2 M NaOH. The organics were extracted with CH_2Cl_2, washed with brine, dried over Na_2SO_4, and concentrated. The resulting yellow oil was placed into a 25-mL round-bottom flask and dissolved in 5 mL of cold ether. HCl (g) was generated and passed into the solution by slow addition of HCl (aq, 12 M) into H_2SO_4 (aq). The resulting white crystals were collected by filtration and dried. The yield was 83%, 140 mg, and the spectral data were $[\alpha]^{24}_D = -110°$ (c = 1, $CHCl_3$); ^{1}H NMR ($CDCl_3$, 300 MHz) δ 7.66 (2H, m), 7.32 (3H, m), 4.14 (1H, m), 3.95 (1H, b), 3.05 (2H, m), 2.60 (3H, d, $J = 4.7$ Hz), 2.29 (4H, m); ^{13}C NMR ($CDCl_3$, 75 MHz) δ 131.99, 129.89, 129.31, 128.76, 73.05, 44.43, 37.67, 31.94, 20.95; HRMS (FAB+) *m/z* calculated for $C_{11}H_{16}N$ [M+]: 162.1283, found 162.1325.

ACKNOWLEDGMENTS. We thank Ariele P. Hanek and Sean M. A. Kedrowski for helpful discussions. This work was supported by the National Institutes of Health (NS 34407; NS 11756) and the California Tobacco-Related Disease Research Program of the University of California, Grant 16RT-0160.

1. Corringer PJ, Le Novere N, Changeux JP (2000) Nicotinic receptors at the amino acid level. *Annu Rev Pharmacol Toxicol* 40:431–458.
2. Grutter T, Changeux JP (2001) Nicotinic receptors in wonderland. *Trends Biochem Sci* 26:459–463.
3. Karlin A (2002) Emerging structure of the nicotinic acetylcholine receptors. *Nat Rev Neurosci* 3:102–114.
4. Gotti C, Zoli M, Clementi F (2006) Brain nicotinic acetylcholine receptors: Native subtypes and their relevance. *Trends Pharmacol Sci* 27:482–491.
5. Romanelli MN, et al. (2007) Central nicotinic receptors: Structure, function, ligands, and therapeutic potential. *ChemMedChem* 2:746–767.
6. Coe JW, et al. (2005) Varenicline: An alpha 4 beta 2 nicotinic receptor partial agonist for smoking cessation. *J Med Chem* 48:3474–3477.
7. Mansvelder HD, Keath JR, McGehee DS (2002) Synaptic mechanisms underlie nicotine-induced excitability of brain reward areas. *Neuron* 33:905.
8. Nashmi R, et al. (2007) Chronic nicotine cell specifically upregulates functional alpha 4* nicotinic receptors: Basis for both tolerance in midbrain and enhanced long-term potentiation in perforant path. *J Neurosci* 27:8202–8218.
9. Tapper AR, et al. (2004) Nicotine activation of alpha4* receptors: Sufficient for reward, tolerance, and sensitization. *Science* 306:1029–1032.
10. Beers WH, Reich E (1970) Structure and activity of acetylcholine. *Nature* 228:917–922.
11. Glennon RA, Dukat M (2000) Central nicotinic receptor ligands and pharmacophores. *Pharm Acta Helv* 74:103–114.
12. Glennon RA, Dukat M, Liao L (2004) Musings on alpha4beta2 nicotinic acetylcholine (nACh) receptor pharmacophore models. *Curr Top Med Chem* 4:631–644.
13. Dougherty DA, Stauffer DA (1990) Acetylcholine binding by a synthetic receptor. Implications for biological recognition. *Science* 250:1558–1560.
14. Xiu X, Puskar NL, Shanata JAP, Lester HA, Dougherty DA (2009) Nicotine binding to brain receptors requires a strong cation-π interaction. *Nature* 458:534–537.
15. Zhong W, et al. (1998) From *ab initio* quantum mechanics to molecular neurobiology: A cation-π binding site in the nicotinic receptor. *Proc Natl Acad Sci USA* 95:12088–12093.
16. Dougherty DA (2008) Cys-loop neuroreceptors: Structure to the rescue? *Chem Rev* 108:1642–1653.
17. Brejc K, et al. (2001) Crystal structure of an ACh-binding protein reveals the ligand-binding domain of nicotinic receptors. *Nature* 411:269–276.
18. Celie PH, et al. (2004) Nicotine and carbamylcholine binding to nicotinic acetylcholine receptors as studied in AChBP crystal structures. *Neuron* 41:907–914.
19. Rucktooa P, Smit AB, Sixma TK (2009) Insight in nAChR subtype selectivity from AChBP crystal structures. *Biochem Pharmacol* 78:777–787.
20. Hansen SB, et al. (2006) Structural characterization of agonist and antagonist-bound acetylcholine-binding protein from *Aplysia californica*. *J Mol Neurosci* 30:101–102.
21. Hansen SB, et al. (2005) Structures of Aplysia AChBP complexes with nicotinic agonists and antagonists reveal distinctive binding interfaces and conformations. *EMBO J* 24:3635–3646.
22. Taylor P, et al. (2007) Structure-guided drug design: Conferring selectivity among neuronal nicotinic receptor and acetylcholine-binding protein subtypes. *Biochem Pharmacol* 74:1164–1171.
23. Cashin AL, Petersson EJ, Lester HA, Dougherty DA (2005) Using physical chemistry to differentiate nicotinic from cholinergic agonists at the nicotinic acetylcholine receptor. *J Am Chem Soc* 127:350–356.
24. Koh JT, Cornish VW, Schultz PG (1997) An experimental approach to evaluating the role of backbone interactions in proteins using unnatural amino acid mutagenesis. *Biochemistry* 36:11314–11322.
25. England PM, Zhang Y, Dougherty DA, Lester HA (1999) Backbone mutations in transmembrane domains of a ligand-gated ion channel: Implications for the mechanism of gating. *Cell* 96:89–98.
26. Deechongkit S, et al. (2004) Context-dependent contributions of backbone hydrogen bonding to beta-sheet folding energetics. *Nature* 430:101–105.
27. Deechongkit S, Dawson PE, Kelly JW (2004) Toward assessing the position-dependent contributions of backbone hydrogen bonding to beta-sheet folding thermodynamics employing amide-to-ester perturbations. *J Am Chem Soc* 126:16762–16771.
28. Gleitsman KR, Kedrowski SMA, Lester HA, Dougherty DA (2008) An intersubunit hydrogen bond in the nicotinic acetylcholine receptor that contributes to channel gating. *J Biol Chem* 283:35638–35643.
29. Fonck C, et al. (7, 2005) Novel seizure phenotype and sleep disruptions in knock-in mice with hypersensitive alpha 4* nicotinic receptors. *J Neurosci* 25:11396–11411.
30. Nowak MW, et al. (1998) *In vivo* incorporation of unnatural amino acids into ion channels in a *Xenopus* oocyte expression system. *Methods Enzymol* 293:504–529.
31. Rodriguez EA, Lester HA, Dougherty DA (2007) Improved amber and opal suppressor tRNAs for incorporation of unnatural amino acids in vivo. Part 1: Minimizing misacylation. *RNA* 13:1703–1714.
32. Rodriguez EA, Lester HA, Dougherty DA (2007) Improved amber and opal suppressor tRNAs for incorporation of unnatural amino acids in vivo. Part 2: Evaluating suppression efficiency. *RNA* 13:1715–1722.
33. Dunsmore CJ, Carr R, Fleming T, Turner NJ (2006) A chemo-enzymatic route to enantiomerically pure cyclic tertiary amines. *J Am Chem Soc* 128:2224–2225.
34. Kash TL, Jenkins A, Kelley JC, Trudell JR, Harrison NL (2003) Coupling of agonist binding to channel gating in the GABA(A) receptor. *Nature* 421:272–275.
35. Price KL, Millen KS, Lummis SC (2007) Transducing agonist binding to channel gating involves different interactions in 5-HT3 and GABAC receptors. *J Biol Chem* 282:25623–25630.
36. Venkatachalan SP, Czajkowski C (2008) A conserved salt bridge critical for GABAA receptor function and loop C dynamics. *Proc Natl Acad Sci USA* 105:13604–13609.
37. Mu TW, Lester HA, Dougherty DA (2003) Different binding orientations for the same agonist at homologous receptors: A lock and key or a simple wedge? *J Am Chem Soc* 125:6850–6851.
38. Torrice MM (2009) *Chemical-Scale Studies of the Nicotinic and Muscarinic Acetylcholine Receptors* (California Institute of Technology, Pasadena, CA).
39. Torrice MM, Bower KS, Lester HA, Dougherty DA (2009) Probing the role of the cation-pi interaction in the binding sites of GPCRs using unnatural amino acids. *Proc Natl Acad Sci USA* 106:11919–11924.
40. Felpin F-X, et al. (2001) Efficient enantiomeric synthesis of pyrrolidine and piperidine alkaloids from tobacco. *J Org Chem* 66:6305–6312.